MR Venography Using BOLD Contrast at 9.4T

S-H. Park[1], S-G. Kim[1]

[1]Brain Imaging Research Center, Dept. of Neurobiology, University of Pittsburgh, Pittsburgh, PA 15203, United States

Introduction

MR venography is important for non-invasive visualization and characterization of vascular structures. The identification of venous vessels is especially critical for avoiding large vessel contributions to fMRI maps. MR venographic images can be obtained using the BOLD effect from deoxyhemoglobin as an intrinsic venous blood contrast agent, as demonstrated by Haacke and his colleagues [1-3]. At lower field strengths of 1.5T and 3.0T, the contrast between veins and tissues was improved by a filtering method using phase information, TE was set to 25~50 ms in order to obtain a phase difference of ~180° between veins and surrounding tissue, and the phase-contrast mask generated from the phase image was multiplied by the magnitude image [1-3]. However, the quality of the venogram is dependent on the choice of scheme for phase-contrast masking and the angle between vessel direction and main magnetic field [2]. At ultrahigh magnetic fields, the phase masking scheme may not be necessary because T_2^* of venous blood is relatively short, compared to tissue T_2^*. At 9.4T, MR signal from veins can be suppressed using TE = 20 - 25 ms, which is ~3 - 4 times the T_2 value of venous blood. In original T_2*-weighted images published by Ogawa [4], venous vessels were visualized using a high-resolution gradient-recalled echo imaging technique. We extended this idea by adapting it to a 3-D imaging technique and applying the minimum intensity projection method. To increase the contrast between tissue and venous vessels, imaging parameters were optimized.

Methods

Experiments were performed on 5 male Sprague-Dawley rats weighing 300~400g. They were intubated and artificially ventilated under 1.5% isoflurane anesthesia in a N_2O/O_2 mixture of 70:30. Their body temperature was maintained at a normal condition by a warm water pad and breathing pattern was monitored throughout the experiment.

A Varian 9.4T MRI system (with 31 cm bore size) was used with a quadrature surface RF coil, which was composed of two circular coils with each size of 1.6 cm diameter. Voxel-localized shimming (PRESS) was performed.

Venographic images were acquired by a flow compensated, T_2*-weighted, low-bandwidth (32~50Hz), 3-D gradient recalled echo pulse sequence. To reduce scan time along both 1st and 2nd phase-encoding directions, 75% of partial Fourier acquisition was used. Typical imaging parameters were as follows: TR = 50 ms, TE = 20 – 25 ms, FOV = 3.0 x 1.5 x 1.5 cm^3, Matrix size = 384 x 192 x 192, flip angle = ~15°, and scan time = 34 min 38 sec. Then, the 3-D dataset was zero-padded to a matrix size of 512 x 256 x 256. Nominal resolution is 58 µm. To visualize a 2-D format from the 3-D dataset, a 16-plane (0.94 mm thick) slab was selected. Minimum intensity projection (mIP) and non-uniformity correction algorithms [5] were applied for better visualization of veins as suggested previously [1,2,3], and for correction of the non-uniform B_1 field of surface coil, respectively.

To determine an optimal echo time for venographic image acquisitions, we performed computer simulation as well as obtained venographic images with different TEs of 12 – 30 ms. Data acquisition bandwidth was adjusted for maximizing signal-to-noise ratios. For computer simulation, published T_1 and T_2 values at 9.4T were used [6-7].

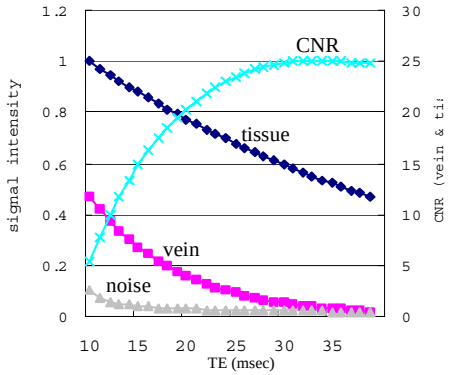

Fig. 1. Simulation results. Tissue signals and noise levels were set to 1.0 and 0.1 at at TE = 10 ms, respectively. a.u.: arbitrary unit

Results and Discussions

Figure 1 shows the simulation results of normalized signal intensity and contrast-to-noise ratio between tissue and vein (CNR) as a function of TE. Since arbitrary units were used here, CNR is a relative value, rather than an absolute one. At longer TE, the tissue signal (gray matter) decayed and noise level also decreased due to lower bandwidth. Thus, the optimal CNR is ~33 ms (Figure 1). However, at longer TE, image artifacts induced by susceptibility effect are more pronounced due to long TE and low bandwidth (Figure 2(e)). Based on our TE-dependent experiments shown in Figure 2, the optimal TE is 20 – 25 ms when considering both overall image quality and CNR between vein and tissues.

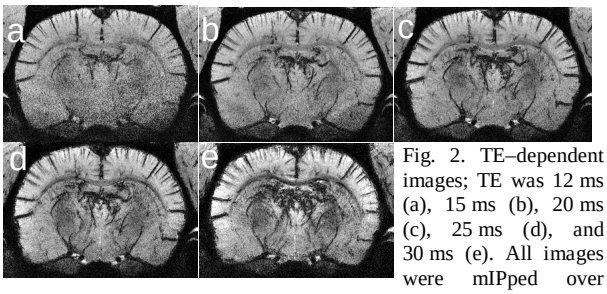

Fig. 2. TE–dependent images; TE was 12 ms (a), 15 ms (b), 20 ms (c), 25 ms (d), and 30 ms (e). All images were mIPped over 0.94 mm

Figure 3 shows representative venographic images of one rat with mIP and non-uniformity correction. The relatively dark region between cortex (Cor) and hippocampus (Hip) is white matter (WM), which is still distinguishable from veins. Dark lines between the cortex and the thalamus indicated by arrows are large draining veins. More importantly, intracortical veins within the cortex and veins within the hippocampus were clearly observed. Since the susceptibility effect induced by deoxyhemoglobin extends beyond vessel walls, the observed vessel size is much larger than the actual diameter. According to the size of intracortical veins measured by vascular histology [8,9], the diameter of the smallest intracortical vein is ~20 µm, which may be detected in our images.

Exquisite venous vessel patterns can be detected at 9.4T. This technique can be easily applied to humans at high magnetic fields such as 7T. Higher magnetic field is advantageous because of shorter T_2 values of veins and higher SNR. Visualization of blood vessels is critical for removing the large vessel contribution from BOLD images, and may be also useful for clinical and developmental brain research.

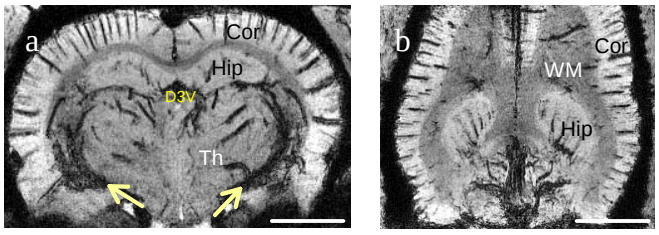

Figure 3. Venograms of one representative animal along coronal (a) and axial (b) directions. Both images were mIPped over 0.94 mm. Cor: cortex, Hip: hippocampus, WM: white matter, D3V : dorsal 3rd ventricle, and Th: thalamus . Yellow arrows: large draining veins. Scale bar: 3 mm.

References

1. Haacke et al. Magn. Reson. Med. 52:612-618 (2004). 2. Reichenbach et al, NMR in Biomedicine 14:453-467 (2001). 3. Reichenbach et al, Radiology 204:272-277 (1997). 4. Ogawa et al. Magn. Reson. Med. 14:68-78 (1990). 5. Cohen et al. Human Brain Mapping 10:204-211 (2000). 6. Tsekos et al., Magn. Reson. Med. 39:564-573 (1998). 7. Lee et al., Magn. Reson. Med. 42:919-928 (1999). 8. Duvernoy et al., Brain Research Bulletin, 7:519-579 (1981). 9. Nakai et al., Stroke 12:653-659 (1981).

Supported by NIH grants (RR17239, EB003324, NS44589, EB003375, EB002013)